Local and Average Diffusion of Nanosolutes in Agarose Gel: The Effect of the Gel/Solution Interface Structure

ARTICLE *in* LANGMUIR · FEBRUARY 2007

Impact Factor: 4.46 · DOI: 10.1021/la0611155 · Source: PubMed

3 AUTHORS, INCLUDING:

Jerome Labille
Centre Européen de Recherche et d'Enseigne…

54 PUBLICATIONS **1,214** CITATIONS

SEE PROFILE

Local and Average Diffusion of Nanosolutes in Agarose Gel: The Effect of the Gel/Solution Interface Structure

Jérôme Labille,*,† Nicolas Fatin-Rouge,‡ and Jacques Buffle

Chimie Analytique et Biophysicochimie de l'Environnement (CABE), Science II (University of Geneva), 30 quai E. Ansermet, CH-1211 Geneva 4, Switzerland

Received April 25, 2006. In Final Form: October 31, 2006

Fluorescence correlation spectroscopy (FCS) has been used to study the diffusion of nanometric solutes in agarose gel, at microscopic and macroscopic scales. Agarose gel was prepared and put in contact with aqueous solution. Several factors were studied: (i) the role of gel relaxation after its preparation, (ii) the specific structure of the interfacial zone and its role on the local diffusion coefficient of solutes, and (iii) the comparison between the local diffusion coefficient and the average diffusion coefficient in the gel. Fluorescent dyes and labeled biomolecules were used to cover a size range of solutes of 1.5 to 15 nm. Their transport through the interface from the solution toward the gel was modeled by the first Fick's law based on either average diffusion coefficients or the knowledge of local diffusion coefficients in the system. Experimental results have shown that, at the liquid/gel interface, a gel layer with a thickness of 120 μm is formed with characteristics significantly different from the bulk gel. In particular, in this layer, the porosity of agarose fiber network is significantly lower than in the bulk gel. The diffusion coefficient of solutes in this layer is consequently decreased for steric reasons. Modeling of solute transport shows that, in the bulk gel, macroscopic diffusion satisfactorily follows the classical Fick's diffusion laws. For the tested solutes, the local diffusion coefficients in the bulk gel, measured at microscopic scale by FCS, were equal, within experimental errors, to the average diffusion coefficients applicable at macroscopic scales ($\geq$mm). This confirms that anomalous diffusion applies only to solutes with sizes close to the gel pore size and at short time ($\leq$min) and spatial scales (≤ 1 μm).

1. Introduction

In rhizospheric or aquatic environment, the fate of elements such as plant nutriments or pollutants highly depends on their interactions with neighboring particulate matter, inducing either transport or storage. Most of the media encountered in such systems are noncrystalline porous and disordered materials, in which transport of nanoparticles is mainly driven by diffusion processes. Among others, the phenomenon of diffusion in bacterial polysaccharidic gels and biofilms is particularly crucial for the bioavailability to plant roots or bacterial flocs of nutrients or pollutants. In addition to this environmental reason, studying the mechanism of diffusion in gels is also of considerable interest for biological,[1] pharmaceutical,[2,3] or analytical[4−6] applications based on it. Restrained diffusion of solutes in gel has been modeled[7−9] and is well documented experimentally for agarose gels.[8,10−12]

In previous works, Fatin-Rouge et al.[12,13] have studied by fluorescence correlation spectroscopy (FCS) the various factors which control the diffusion of solutes in agarose gel. They modeled the contributions of steric, electrostatic, and chemical effects to diffusion.[12] They have estimated the largest pore size in the bulk gel and pointed out that anomalous diffusion can occur for particles with sizes similar to the pore size.

Comparison between diffusion coefficients at microscopic ($\leq\mu$m) and macroscopic scales (≥ 100 μm), however, has never been done in agarose. In addition, since the cohesion of agarose gel largely depends on physical aggregation forces between agarose fibers, it can be expected that the internal structure of the bulk gel is different from that in contact with neighboring gas or liquid phase. Indeed, at the interface, gel fibers should be organized differently to ensure sufficient cohesive forces. As a consequence, diffusion properties in the gel part of the interface might be quite different from those in the bulk phase, which may have a major impact on the diffusive transport of solutes from the liquid phase to the gel.

In this context, the aim of this work is to study the diffusion properties of solutes, at the gel/water interface as well as in the bulk of agarose gel, to compare microscopic and macroscopic behaviors. The final goal is to evaluate the impact of these effects on the average flux of solutes from the solution through the whole gel.

In the following, the term interface will refer to the limit between the gel and air or solution phase, while the word

* Corresponding author. E-mail: labille@cerege.fr. Fax: 33(0) 442 97 15 59.

† Present address: CEREGE/CNRS, Europole Méditerranéen de l'Arbois, BP80, 13545 Aix en Provence, France.

‡ Present address: Laboratoire de Chimie des Matériaux et Interfaces, Université de Franche-Comté, 16 route de Gray, 25030 Besançon cedex, France.

(1) Ottenbrite, R. M.; Huang, S. J. *Hydrogels and biodegradable polymers for biological applications*; Park, K., Ed.; American Chemical Society: Washington, DC, 1996.

(2) De rossi, D.; Kajiwara, K.; Osada, Y.; A. Y. *Polymer gels*; Plenum Press: New York, 1991.

(3) Lacroix-Gueu, P.; Briandet, R.; Leveque-Fort, S.; Bellon-Fontaine, M. N.; Fontaine-Aupart, M. P. *Cr. Biol.* **2005**, *328*, 1065−1072.

(4) Buffle, J.; Tercier-Waeber, M. L. *Trac-Trend Anal. Chem.* **2005**, *24*, 172−191.

(5) Buffle, J.; Horvai, G. In *IUPAC Series in analytical and Physical Chemistry of Environmental Systems*; Wiley: Chichester, 2000.

(6) Davison, W.; Zhang, H. *Nature* **1994**, *367*, 546−548.

(7) Amsden, B. *Polym. Gels Networks* **1998**, *31*, 13−43.

(8) Fatin-Rouge, N.; Wilkinson, K.; Buffle, J. *J. Phys. Chem. B* **2006**, *110*, 20133−20142.

(9) Guiot, E.; Georges, P.; Brun, A.; Fontaine-Aupart, M. P.; Bellon-Fontaine, M. N.; Briandet, R. *Photochem. Photobiol.* **2002**, *75*, 570−578.

(10) Jonhson, E. M.; Berk, D. A.; Jain, R. K.; Deen, W. M. *Biophys. J.* **1996**, *70*, 1017−1023.

(11) Pluen, A.; Netti, P. A.; Rakesh, K. J.; Berk, D. A. *Biophys. J.* **1999**, *77*, 542−552.

(12) Fatin-Rouge, N.; Milon, A.; Buffle, J.; Goulet, R. R.; Tessier, A. *J. Phys. Chem. B* **2003**, *107*, 12126−12137.

(13) Fatin-Rouge, N.; Starchev, K.; Buffle, J. *Biophys. J.* **2004**, *86*, 2710−2719.

10.1021/la0611155 CCC: $37.00
Published on Web 12/24/2006

interphase will be used to denote the layers of solution and gel in which concentrations of solutes and phase structures are different from the bulk solution or gel.

2. Theory

2.1. Fluorescence Correlation Spectroscopy Measurements. FCS was used to measure the diffusion coefficient of fluorescent solutes and nanometric particles in both aqueous solution and agarose gels. These measurements are based on the recording of the intensity fluctuations of light emitted from a small number of molecules or particles diffusing freely through a micrometric confocal sample volume (SV) located in a laser beam.[14,15] The size of the SV is limited by the approximately Gaussian radial profile of the laser beam intensity and the focal length of the optics. Its transverse radius, ω_z, is about 300 nm, and its half-height, ω_{xy}, is 1500 nm. Variations in fluorescence intensity in the SV were analyzed using the auto-correlation function (ACF), $G(\tau)$,[16] corresponding to the free diffusion of a single species:

$$G(\tau) = \frac{(1 - F_{tr} + F_{tr}\exp(-\tau/\tau_{tr}))}{2\sqrt{2}N(1 - F_{tr})} \frac{1}{(1 + (\tau/\tau_c))(1 + (\tau/p^2\tau_c))^{0.5}} \quad (1)$$

where F_{tr} is the triplet fraction, τ_{tr} is the triplet lifetime, τ is the delay-time, τ_c is the characteristic mean time spent by fluorescent molecules or particles in the SV, N is their mean number in the SV, and $p = \omega_z/\omega_{xy}$. In a fully isotropic microenvironment around the confocal volume, the diffusion coefficient, D, of solutes can be simply obtained from the following equation:[16]

$$D = {\omega_{xy}}^2/4\tau_c \quad (2)$$

2.2 Modeling Macroscopic Diffusion in Gel. In uniform Euclidean media, at sufficiently large time and space scales,[17] the random diffusion motion of a solute is described by[18]

$$\overline{x^2(t)} = \Gamma t^{2/d_w} \quad (3)$$

where $\overline{x^2(t)}$ is the mean square displacement of the diffusing solute, t is time, Γ is a transport coefficient, and d_w is the fractal dimension of the diffusion path. Indeed the random walk of a diffusing solute is statistically self-similar at different scales and can be represented by means of the fractal concepts. In homogeneous media, $d_w = 2$, Einstein's relation (eq 4) modeling Brownian motion is valid, and diffusion is said normal. In gels, the diffusive properties of a solute depend on one hand on the spatial and time scales of observation, and on another hand on the relative sizes of the solute and the gel pores. When the former is not very small compared to the latter, particle diffusion is delayed by obstruction. Then, $d_w > 2$, which corresponds to the slowing down of the transport with regard to normal diffusion. The diffusion law then becomes "anomalous".[19−21]

In the present work, considering the large spatial (mm) and time scales (min to hours) used for macroscopic observations, we shall start with the assumption that the Einstein's relation is valid for the macroscopic description of solute diffusion, both in solution and in bulk gel. Comparison with local, microscopic measurements by FCS will enable us to check whether this assumption is valid in the μm to mm range.

For normal diffusion ($d_w = 2$), eq 3 thus becomes

$$\overline{x^2(t)} = 2dDt \quad (4)$$

where d is the spatial dimension, and Fick's second law holds:

$$\frac{\partial C_w}{\partial t} = D_w \frac{\partial^2 C_w}{\partial x^2} \quad (5)$$

where $C_w(x, t)$ is the solute concentration in the water phase, D_w the diffusion coefficient in water, t the time, and x the distance. The same equation is applicable for diffusion in the gel, by changing $C_w(x, t)$ and D_w by $C_g(x, t)$, and D_g, i.e. the concentration and diffusion coefficient of the solute in the gel. Note that, depending on conditions, D_w and D_g may also be functions of x. They should then be introduced in the differentials. Below, the system will be considered as composed of two semi-infinite phases, with the following boundary conditions at the interface, valid when both the gel and solution are homogeneous:

(i) The partition coefficient, K, of the solute between gel and water is given by

$$K = \frac{C_g(t)}{C_w(t)} \quad (6)$$

It is thus assumed that a quick partitioning equilibrium always exists at the interface. The physicochemical factors which may influence K are discussed in ref 12.

(ii) The fluxes of solutes at the interface, on the gel and water sides, are equal, i.e., for diffusion coefficients independent of x:

$$D_g\left(\frac{\partial C_g(x, t)}{\partial x}\right)_{x=0} = D_w\left(\frac{\partial C_w(x, t)}{\partial x}\right)_{x=0} \quad (7)$$

When D_g (or D_w) vary with x, $C_g(x, t)$ must be computed rigorously by numerical resolution, by introducing the experimental functions $D_g(x)$ (or $D_w(x)$) measured for instance by FCS, in the differentials of eqs 5 and 7. This has been done in Section 4.3. It should be noted that variation of D_g with x is usually due to nonhomogeneity of the gel. Then K is also a function of x, $K(x)$.

On another hand, approximate values of D_w, D_g, and K, for a given distance x, $\tilde{D}_w(x)$, $\tilde{D}_g(x)$, and $K(x)$, can be obtained by using the analytical solution of eqs 5−7[22] and by assuming that the values of , $\tilde{D}_w(x)$, $\tilde{D}_g(x)$, and $K(x)$ are constant in the range $0-x$.

$$C_w(x, t) = \frac{C_w^0}{1 + K\sqrt{\tilde{D}_g/\tilde{D}_w}} \cdot \left[1 + K\sqrt{\tilde{D}_g/\tilde{D}_w}\ \mathrm{erf}\left(\frac{|x|}{2\sqrt{\tilde{D}_w t}}\right)\right] \quad (8)$$

$$C_g(x, t) = \frac{C_w^0 K}{1 + K\sqrt{\tilde{D}_g/\tilde{D}_w}} \cdot \left[1 - \mathrm{erf}\left(\frac{x}{2\sqrt{\tilde{D}_g t}}\right)\right] \quad (9)$$

where C_w^0 is the initial concentration of solute in the water phase. As the solute diffuses in the gel, concentration profiles are formed. They can be represented by the corresponding fluorescence intensity profiles determined experimentally. Provided the

(14) Rigler, R.; Mets, U.; Widengren, J.; Kask, P. *Eur. Biophys. J. Biophy.* **1993**, *22*, 169−175.
(15) Widengren, J.; Rigler, R. *Cell. Mol. Biol.* **1998**, *44*, 857−879.
(16) Aragon, S. R.; Pecora, R. *J. Phys. Chem. B* **1975**, *64*, 1791−1803.
(17) Lyklema, J. In *Fundamentals of Colloid and Interface Science*; Academic Press: London, 1991; Vol. 1, pp 674.
(18) Havlin, S.; Ben-Avraham, D. *Adv.Phys.* **1987**, *36*, 695−798.
(19) Havlin, S.; Ben-Avraham, D. *Adv. Phys.* **2002**, *51*, 187−292.
(20) Saxton, M. J. *Biophys. J.* **2001**, *81*, 2226−2240.
(21) Saxton, M. J. *Biophys. J.* **1994**, *66*, 394−401.
(22) Crank, J. *The Mathematics of Diffusion*, 2nd ed.; Clarendon Press: Oxford, England, 1975.

absorbance A in solution and gel phases is small at the excitation wavelength used, λ_{exc}, ($A(\lambda_{exc}) \leq 0.05$)[23] and no inner postfilter effect occurs, the fluorescence intensity, I_g, of the solute in the gel is given by

$$I_g = k_g I_0 (1 - 10^{-\epsilon_g l C_g}) \sim 2.3 k_g I_0 \epsilon_g l C_g \qquad (10)$$

where I_0 is the intensity of the excitation beam at the entrance of the confocal volume, ϵ_g is the molar absorptivity of the solute in the gel, l is the path length (i.e. ω_z), and k_g is a constant factor relating the fluorescence intensity to the absorbed intensity. The same equation can be used with subscripts "w", to relate the fluorescence intensity in the water phase, I_w, to the corresponding concentration C_w.

It follows that

$$\frac{C_g(x, t)}{C_w^0} \sim \frac{k_w \epsilon_w I_g(x, t)}{k_g \epsilon g I_w^0} \qquad (11)$$

where I_w^0 is the fluorescence intensity emitted from the water phase at the beginning of the transport measurement, when the solute is introduced in this phase. Combining eqs 9 and 11, one gets

$$I_g(x, t) \sim \frac{\gamma I_w^0 K}{1 + K\sqrt{\tilde{D}_g/\tilde{D}_w}} \left[1 - \mathrm{erf}\left(\frac{x}{2\sqrt{\tilde{D}_g t}}\right)\right] \qquad (12)$$

with $\gamma = (k_g \epsilon_g)/(k_w \epsilon_w)$.

I_w^0 and the values of $\tilde{D}_g$ and K for a fixed distance x were obtained by nonlinear least-squares fits of experimental time-dependent fluorescence intensities recorded at positions x from the interface, by minimizing the function

$$\chi^2 = \sum_{j=1}^{n} [I_g^{exp}(x, t) - I_g^{calc}(x, t)]^2 \qquad (13)$$

The values of $\tilde{D}_g$ and K are compared below to the exact values of $D_g(x)$ measured experimentally, at microscopic scale, by FCS.

3. Experimental Section

3.1. Fluorescence Correlation Spectroscopy. The FCS apparatus used in these experiments to measure locally the diffusion coefficients within the gel is a ConfoCor Axiovert 135 TV from Carl Zeiss (Germany). The samples were excited with an Ar^+ laser (488 or 514 nm), and fluorescence intensity was measured with an avalanche photodiode detector (SPCM-200PQ).

Values of p were obtained by calibration of the apparatus with Rhodamine R6G fluorophore (Sigma-Aldrich 99%), which has a known diffusion coefficient $D^{R6G}{}_w$ of 2.8×10^{-6} cm^2 s^{-1} in water.[24]

3.2. Agarose Gel Preparation. Agarose is a linear polysaccharide constituted of agarobiose repeating units, isolated from Agar red algae *Rhodophyta*. Purified agarose powder was obtained from Biofinex (Switzerland) (LGL, molecular biology grade, lot no. 8041), and used without further treatment. The temperature of phase transition of aqueous agarose is around 60 °C.[25] The powder is dissolved above this temperature. By cooling below 60 °C, the solution gels by physical aggregation of macromolecules in a continuous network. A stock of hot agarose solution of 2 wt % was first prepared in Milli-Q water by heating at 90−100 °C, until total dissolution of agarose powder, and let for at least 2 h in an oven at 75 °C. Agarose samples were then diluted with appropriate volumes of hot phosphate buffer (pH 6.8) and Milli-Q water, so as to reach

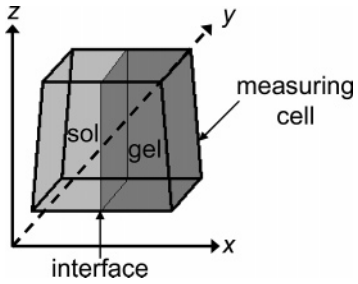

Figure 1. Schematic drawing of the measuring cell containing the agarose gel in contact with solution (sol). The interface between each phase is shown by the arrow.

1.5 wt % solutions and an electrolyte concentration of 3×10^{-2} M or 10^{-4} M. A total of 350 μL of hot agarose solution was introduced in the 700 μL FCS measurement cell, in such a way that the agarose/air interface was exactly flat and perpendicular to the movable (xy) plane of the FCS measurement platform (Figure 1). A special device was built in our laboratory to prepare a well-controlled interface. The hot solution was then let to gel by cooling in closed atmosphere saturated with H_2O vapor preventing dehydration, particularly at the gas−gel interphase. The cooling rate was either 10 mn at ambient temperature or 30 mn in a water bath initially heated at 75 °C (slow cooling rate). The gel was then let to relax from 0 to 4 h (usually 3 h unless otherwise stated). Finally a buffer solution with the same electrolyte concentration and pH as that in the gel was placed in the FCS cell, in contact with the gel (Figure 1).

3.3. Agarose Gel Stability Studied by Means of Fluorescent Labeled Gel. In order to better understand the effect of cooling rate and relaxation time on the stability of the gel, the latter was prepared with agarose labeled with the fluorescent dye Rhodamine 123 (R123, Acros Organics, France). The release of the agarose fibers from the gel to the solution was then followed by FCS.

The labeling procedure is based on the reaction between the aldehyde group of the open terminal ose of the macromolecule and the amine group of the Rhodamine 123, which induces imine formation.[26] For this purpose, an appropriate volume of R123, corresponding to 5 equiv per agarose molecule, was dissolved in a small volume of methanol and introduced in a large volume of hot agarose solution. In a second time, the imine group is stabilized by its reduction to amino group, by addition of an excess of $NaCNBH_3$ (purum, Acros). After cooling, the excess of Rhodamine 123 in the gel was eliminated by cutting the gel into 5 mm edge cubes and submitting them to many washing cycles in ethanol solution as follows. The cubes in ethanol were heated to liquefy, cooled down to gel again, cut into cubes, and washed copiously with ethanol several times, to remove the free Rhodamine. A few cubes of this clean and highly fluorescent agarose gel were then added to water in the preparation of a new agarose stock solution, in order to finally get a gel with appropriate fluorescence, in the desired buffer. The release to the solution of agarose fibers from this gel was measured by FCS (Figure 2). This release probably results from the free diffusion of a small proportion of fibers nonaggregated or weakly bound to the fiber network of the gel. The existence of weakly bound fibers in the gel is expected since gel formation is based on physical aggregation and not covalent binding of the fibers. The statistics of aggregation and the presence of negatively charged pyruvate groups in agarose, which create electrostatic repulsions between fibers, will thus result in the presence of free fibers in the network.

It appeared that fiber release decreases drastically when the relaxation time increases until 3 h (Figure 2a). This suggests that the gel is not yet fully stabilized before 3 h of relaxation, and that the aggregation process is still continuing at this time with very slow kinetics. This is coherent with the weak attractive interactions between agarose fibers, due to electrostatic repulsions, in particular at low ionic strength (10^{-4} M), where a higher fiber release is also observed

(23) Fery-Forgues, S.; Lavabren, D. *J. Chem. Ed.* **1999**, *76*, 1260−1264.
(24) Magde, E. L.; Elson, E. L.; Webb, W. W. *Biopolymers* **1974**, *13*, 29−61.
(25) The Agarose Monograph; FMC Bioproducts: Rockland, ME, 1982.
(26) Meunier, F.; Wilkinson, K. J. *Biomacromolecules* **2002**, *3*, 857−864.

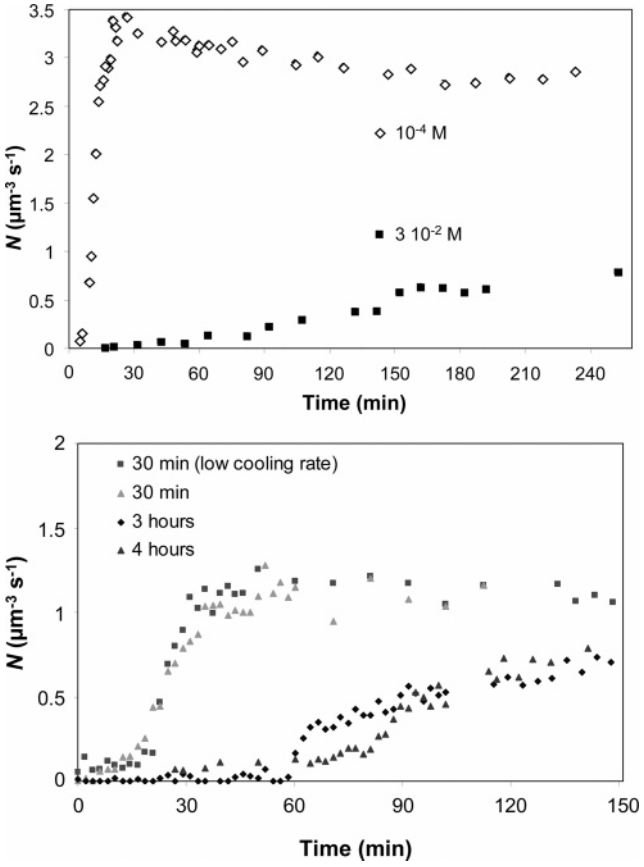

Figure 2. Release of labeled agarose fibers from gel to solution (expressed as the mean number of molecules N in the sample volume SV during the delay time, τ); (2a) for two ionic concentrations, in phosphate buffer at pH = 6.8 with a relaxation time fixed at 30 min; (2b) for relaxation times of 30 min (regular and slow cooling rates), 3 h, or 4 h (phosphate buffer: pH = 6.8, $I = 10^{-4}$ M).

compared to high ionic strength (3×10^{-2} M) (Figure 2b). On the other hand, no effect of the cooling rate was observed on the release of agarose fibers (Figure 2b). In the following, all measurements were thus made with gels prepared in optimal conditions to favor fiber aggregation, i.e., by using a preparative ionic strength of 3×10^{-2} M and a relaxation time of 3 h.

3.4. Diffusing Solutes. The following solutes were used to study the diffusion properties at the interface and in the bulk gel. They were chosen because of their size range (see hydrodynamic radius below) and because previous work[13] has shown that they do not interact chemically in the gel: Rhodamine R6G (0.76 nm, Sigma-Aldrich 99%), protein Parvalbumin (1.87 nm, alexa-488-labeled, Molecular Probes), protein R-phycoerythrin (4.56 nm, TRITC-labeled, Molecular Probes), polystyrene latex microspheres internally labeled with fluorescent dyes (14 nm, R25, Duke Scientific Corp), and three dextrans (polysaccharides with molecular weights (M_w) = 10 000, 40 000, 464 000, $R_h \sim 3.58, 5.93, 13.5$ nm, Sigma Aldrich) labeled in our laboratory with Rhodamine R123, according to the same procedure as that described in Section 3.3 for the agarose labeling (see also ref 26). In spite of a series of rinsing to eliminate the excess of R123 from the labeled dextran, a small fraction of free R123 fluorophore remains in solution. Moreover, it has been observed (data not shown) that, during the labeling procedure, small size hydrolysis fragments are produced which are not easily separated from the test dextrans. FCS measurements should then be corrected to eliminate the contributions of free R123 and dextran fragments. This was performed by transforming the ACF, $G(\tau)$, given by eq 1, to take into account the presence of three diffusing compounds with three different diffusion times:[27]

$$G(\tau) = \frac{(1 - F_{tr} + F_{tr}\exp(-\tau/\tau_{tr}))}{2\sqrt{2}N(1 - F_{tr})}A \qquad (14)$$

$$A = \frac{1 - F - G}{(1 + \tau/\tau_c^{R123})(1 + \tau/p^2\tau_c^{R123})^{0.5}} + \frac{F}{(1 + \tau/\tau_c^{F})(1 + \tau/p^2\tau_c^{F})^{0.5}} + \frac{G}{(1 + \tau/\tau_c^{G})(1 + \tau/p^2\tau_c^{G})^{0.5}}$$

F is the fraction of R123 attached to the test dextran, G is the fraction of R123 attached to dextran fragments and $(1 - F - G)$ is the fraction of free R123. τ_c^F, τ_c^G, and τ_c^{R123} are the respective diffusion times of these three compounds in the gel. τ_c^{R123} is easily measured in a separate experiment, and τ_c^F can be measured by letting the three-component mixtures to diffuse in the gel. Because the test dextran diffuses more slowly than the others, it can be differentiated from the fragments by measuring the macroscopic diffusion of the mixture as a function of time and distance. F, G, and τ_c^G are obtained by fitting the experimental ACF with eq 14. The values of F and τ_c^F enable us to compute specifically the fluorescence intensity (and thus the concentration) of the test dextrans in the gel, at each distance x and time t, as well as the corresponding values of D_g (see Table 1 for bulk gel values).

3.5. Local High Resolution Measurements of Diffusion Coefficients and Comparison with Macroscopically Determined Diffusion Coefficients. In order to study the local structure of the gel at the interphase, the diffusion properties of colloids were measured at micrometric resolution in this region, as function of the distance to the interface. To study the roles of both steric and electrostatic factors, the measurements were performed at ionic strength of 1×10^{-4} and 3×10^{-2} M.[12] A small amount of fluorescent dye R6G was introduced in the hot agarose solution during the gel preparation procedure, just before cooling, so that the fluorophore was homogeneously present in the gel formed in the measurement cell. The same concentration of R6G was also added to the solution in contact with gel. One night of equilibration was used to get homogeneous concentrations of R6G both in gel and solution. The hydrodynamic radius of R6G molecule being much lower than the average pore size of the gel,[13] eqs 1 and 4 can be used to determine the local value of $D_g^{R6G}(x)$, as a function of the distance x to the interface.

Local high-resolution diffusion coefficients of solutes were compared to macroscopic diffusion coefficient values measured as follows. Experiments were made with a buffered solution (phosphate 3×10^{-2} M) at pH = 6.8 and with 1.5 wt % agarose gel. FCS measurements were recorded after a known concentration, C_w, of fluorescent solute was introduced in the solution phase at time t_0 and let to diffuse through the gel phase (Figure 1). Local ($\sim 1\ \mu m^3$) FCS measurements were performed as function of both distance from the interface and time. Local values of N, τ_c, and D_g were obtained from eqs 1 and 2 whereas approximate macroscopic diffusion coefficient values were computed from experimental $I_g(x, t)$ values and eq 12.

4. Results and Discussion

4.1. Solute Diffusion at the Interphase. The diffusion coefficient of R6G at any distance of the solution/gel interface, normalized to the diffusion coefficient of R6G in solution at infinite distance from the interface, $D(x)/D_w(-\infty)$, is shown in Figure 3. The evolution of $D(x)/D_w(-\infty)$ shows a very sharp minimum at the gel/liquid interface, characterized by an abrupt decrease from the bulk solution to the interface on the one hand and a progressive increase from the interface to the bulk gel on the other hand, over a thickness of $\sim 120\ \mu m$. In the gel side, the change of $D(x)$ indicates a lower porosity near the interface than

(27) Schwille, P.; Haupts, U.; Maiti, S.; Webb, W. W. *Biophys. J.* **1999**, *77*, 2251−2265.

Table 1. Hydrodynamic Radius (R_h) Calculated from D_w by the Stokes−Einstein Relationship, Microscopic Diffusion Coefficient in Solution ($D_w(\infty)$) and in the Bulk Gel (D_g(bulk)), and Average (Macroscopic) Diffusion Coefficient in the Bulk Gel, $\bar{D}_g$ Calculated from Equation 4 and Figure 5[a]

	R6G	parvalbum ine	R-phyco.	Dx 10000	Dx 40000	Dx 464000
R_h	0.76	1.87 ± 0.11	4.56 ± 0.3	3.74 ± 0.29	5.81 ± 0.44	
$D_w(-\infty)$	2.8	1.14 ± 0.07	0.47 ± 0.03	0.57 ± 0.05	0.37 ± 0.03	0.16 ± 0.01
D_g(bulk)	2.64 ± 0.015	1.05 ± 0.02	0.386 ± 0.04	0.489 ± 0.008	0.306 ± 0.02	0.116 ± 0.0069
D_g(bulk)/$D_w(\infty)$	0.943 ± 0.005	0.921 ± 0.13	0.791 ± 0.12	0.88 ± 0.13	0.83 ± 0.12	0.71 ± 0.09
$\bar{D}_g$	2.78 (+ 0.43/−0.32)	1.07 (+ 0.26/−0.16)	0.366 (+ 0.05/−0.09)	0.597 (+0.45/−0.18)	0.371 (+0.20/−0.09)	0.073 ± 0.003

[a] The values of diffusion coefficients are expressed as 10^{-6} cm^2 s^{-1}. Measurements were realized in phosphate buffer (pH = 6.8, $I = 3 \times 10^{-2}$ M, $T = 20$ °C).

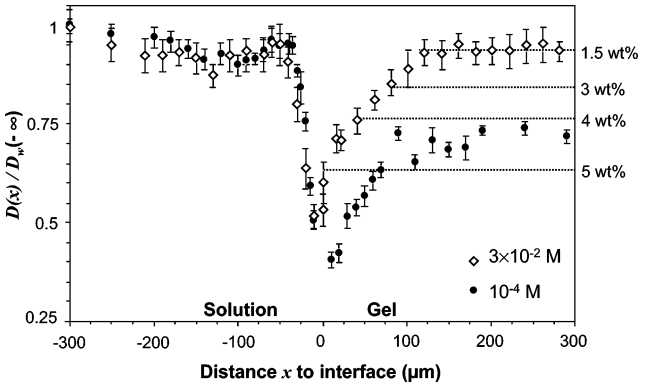

Figure 3. Diffusion coefficient, $D(x)$, of R6G in solution and in the gel, as a function of the distance x from the interface, and of the ionic strength (phosphate buffer, pH = 6.8). Data are normalized by the diffusion coefficient of R6G in solution at infinite distance from the interface, $D_w(-\infty) = 2.8 \times 10^{-6}$ cm^2 s^{-1}. Scattered lines show the average values of D_g(bulk)/$D_w(-\infty)$ measured in reference gels prepared at 1.5, 3, 4, and 5 wt % for $I = 3 \pm 10^{-2}$ M.

in the bulk gel. This cannot be due to a faster dehydration of agarose at the interface, since closed atmosphere saturated with H_2O vapor was always used for preparations. Comparison of $D_g(0 < x < 100\ \mu m)$ values at 3×10^{-2} M ionic strength for an overall 1.5 wt % gel to D_g(bulk) values measured in gels prepared at 3, 4, 5 wt % in the same buffer shows that, close to the interface of an overall 1.5 wt % gel, the diffusion properties of R6G are equivalent to those in the bulk of a 5−6 wt % gel, which corresponds to a very dense gel. The observed decrease of D_g in the interphase may be due to a different structure of the network of agarose fibers, or to a larger fiber concentration, possibly to ensure the cohesive forces required to maintain the gel/solution interface. A detailed discussion of the diffusive properties of the interphase, however, would require a detailed physical chemical study which is out of the scope of this paper. The important point is that the local porosity at the interphase seems to be much lower than in the bulk. Thus the gel side of the interphase may behave as a sieve retaining colloids which would otherwise diffuse in the bulk of the gel. As shown by Fatin-Rouge et al.,[13] colloids with radius of ≥70 nm are blocked in the bulk of agarose gel. The present results suggest that colloids even smaller are not allowed to penetrate the gel, due to the sieving interphase. Indeed, experiments not presented here showed that polystyrene miscrospheres with 14 nm radius could not penetrate the gel through the interface, while they were able to diffuse in the bulk gel when directly introduced before the agarose cooling. On the other hand, dextran macromolecules with a similar hydrodynamic radius (13.5 nm) are able to pass the interface (Section 4.2). The different behavior of latex and dextran may be related to the charge of the former and the flexible conformation of the latter.[11] Anyway, these results suggest that the maximum critical radius for the penetration of solutes at the interphase is close to 14 nm.

The change of $D_g(x)/D_w(-\infty)$ with distance, at 10^{-4} M ionic strength (Figure 3), shows a similar trend as that observed at 3×10^{-2} M, but with a significant shift toward lower values of $D_g(x)/D_w(-\infty)$ at any distance in the gel (e.g., from 0.93 at 3×10^{-2} M to 0.7 at 10^{-4} M, in the bulk). Such a decrease is in good agreement with the role of electrostatic interactions on the diffusion coefficient in gels, as described in ref 12. Indeed it has been clearly shown that interactions between the negatively charged agarose network and positively charged diffusing species (like R6G) lead to a decreased D_g as compared to the value in neutral gel. This electrostatic effect largely increases by decreasing the ionic strength. The fact that the change of $D_g(x)/D_w(-\infty)$ with distance is similar at both ionic strengths suggests that the electrostatic effect on diffusion coefficient is similar in the bulk gel and in the interphase. This would favor the hypothesis that gel fibers are not more concentrated in the interphase but rather locally arranged in a more entangled structure.

In the liquid phase, at both ionic strengths, an interphase layer of ∼30 μm is also formed in contact with the gel. In this layer, $D_w(x)/D_w(-\infty)$ sharply decreases from the bulk solution value to significantly smaller values in the domain $-30\ \mu m < x < 0$ (Figure 3). Such a decrease is attributed to the presence of agarose fibers partly attached to the gel, and partly extending in solution, thus forming a bristling layer. Simultaneously, in this layer, the concentration of fibers released from the gel and diffusing freely in solution, is much larger than in the bulk solution. In such a layer, the viscosity may increase significantly and thus $D_w(x)$ may be significantly lower than $D_w(-\infty)$. The fact that exactly the same trend is observed at both low and high ionic strengths (Figure 3) suggests that the electrostatic effects of charged agarose fibers, in the aqueous interphase layer, is negligible.

4.2. Average Macroscopic Diffusion Coefficients of Solutes in the Gel. Average diffusion coefficients, $\tilde{D}_g$, of solutes in the gel can be determined by recording the fluorescence intensity of the solute as function of time t at different distances x in the gel, during the diffusion process of the solute, from the solution to the gel. This is discussed below, for solutes with different sizes.

Experimental curves of fluorescence intensity as function of time, at different distances x from the interface, are given in Figure 4 for R-phycoerythrin. Similar curves were obtained for the other solutes. Six distances were studied: $-189\ \mu$m in solution, and 50, 300, 550, 800, and 1050 μm in the gel phase. In the bulk solution ($x = -189\ \mu$m), the fluorescence intensity slightly decreases with time, and reaches a plateau about 20% below its initial value, due to the consumption by the gel. At each distance studied in the gel, there is a characteristic time, $t_c(x)$, after which the fluorescence intensity starts to increase, until it reaches a plateau of maximum value. The evolution of $t_c(x)$ is reported in Figure 5, for all types of nanoparticles studied. The vertical dashed line represents the limit, at $x = 120\ \mu$m, separating the bulk gel from the interphase gel layer, which includes the point at 50 μm.

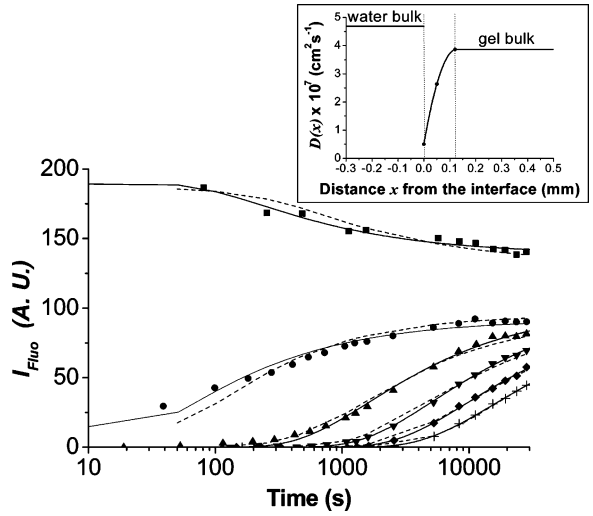

Figure 4. Fluorescence intensity profiles for R-phycoerythrin as a function of time at different positions, x, from the interface: $x = -189$ μm (■), 50 μm (●), 300 μm (▲), 550 μm (▼), 800 μm (◆) and 1050 μm (+). $V_{gel} = 0.35$ mL; $V_{solution} = 0.20$ mL; $T = 20$ °C; phosphate buffer (pH = 6.8, $I = 3 \times 10^{-2}$ M). Solid lines are the fits obtained with eqs 8 and 12 by assuming that K and $\tilde{D}_g$ are independent of time and constant in the domain $0-x$. Different $\tilde{D}_g$ values may be obtained for different values of x (Table 2). Dashed lines: fit obtained by numerical resolution of eq 5, by assuming that K is constant across all the gel phase and by using the following diffusivity profile determined experimentally and shown in Figure 7b. The inset presents the diffusivity profile determined experimentally: $D_w(x) = 4.684 \times 10^{-7}$ cm^{2}s^{-1} for $x < 0$; $D_g(x) = 5 \times 10^{-8} + 5.29456 \times 10^{-5}x - 2.06 \times 10^{-3}\,x^2$ cm^{2}s^{-1} for $0 \le x < 120$ μm; and $D_g(x) = 3.866 \times 10^{-7}$ cm^2 s^{-1} for $x > 120$ μm.

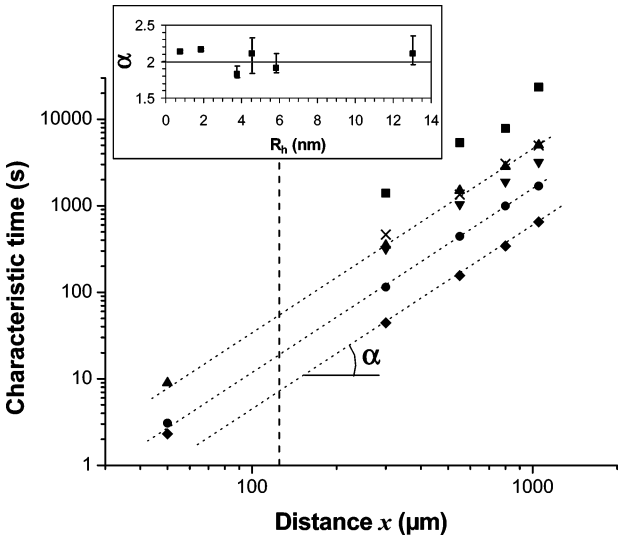

Figure 5. Characteristic diffusion times of solutes in gel as a function of the distance x to the interface; R6G (◆), parvalbumin (●), R-phycoerythrin (▲), dextran 10000 (▼), dextran 40000 (×), dextran 464000 (■). The vertical dashed line indicates the approximate limit between the gel interphase layer and the bulk gel. Electrolyte = phosphate buffer: pH = 6.8, $I = 3 \times 10^{-2}$ M. The inset presents the evolution of the slope α (eq 15) of the lines of Figure 5, as a function of the solute size.

For all profiles located in the bulk gel ($x > 120$ μm), the following relationship holds:

$$t_c(x) = x^{\alpha} \qquad (15)$$

Within experimental errors, for all solutes studied, $\alpha \approx 2$ (inset of Figure 5) which matches well the exponent of normal diffusion (eq 4) related to classical Einstein's relation. This suggests that, for the long time scale studied here, the gel bulk can be treated as homogeneous, with $d_w = 2$ (eq 3), and that the diffusion properties of each solute can be characterized by an average diffusion coefficients, $\bar{D}_g$, and classical Fick's laws. The average macroscopic diffusion coefficients of each solutes, $\bar{D}_g$ calculated from Figure 5 and eq 4 are in reasonable agreement with the values measured at the microscopic scale, D_g(bulk) (Table 1). Moreover, these values also match, and thus validate, the theoretical predictions proposed by Fatin-Rouge et al.[13] by using a model combining obstruction[28] and hydrodynamic[29,30] theories of diffusion in porous media, a mean characteristic fiber radius of 4.1 nm, and a size distribution of the gel pores obtained from small angle neutron scattering measurements.[8]

Table 2. Partition Coefficients (K) and Average Diffusion Coefficients for R-Phycoerythrin in Agarose Gel ($\tilde{D}_g$) Obtained from Experimental Data of Figure 4 and the Approximate Model (Eqs 8−12)[a]

x (μm)	K[b]	$\tilde{D}_g(x)$ or $\tilde{D}_w(x)$ $\times 10^6$ (cm^2 s^{-1})[b]	$\tilde{D}_g(x)/D_w(-\infty)$ or $\tilde{D}_w(x)/D_w(-\infty)$	$\gamma I_{w,0}$[c]
−189	0.462	0.306	0.654	−
50	0.585	0.204	0.436	219
300	0.603	0.274	0.585	249
550	0.602	0.286	0.611	258
800	0.594	0.329	0.703	254
1050	0.568	0.351	0.750	255

[a] See Section 4.3.1 for discussion. pH = 6.8 (phosphate buffer); I = 0.09 M; $T = 20$ °C. $D_w^{R-phyco} = 4.68 \times 10^{-11}$ m^2 s^{-1}. [b] ±10%. [c] $I_{w,0} = 190$.

Inside the interphase ($0 < x < 120$ μm) the values of t_c obtained at $x = 50$ μm (Figure 5) are not in line with their respective series, but shifted toward longer characteristic times. This reflects a lower average macroscopic diffusion coefficient than in the bulk gel, in accordance with the lower microscopic diffusion coefficient measured in Figure 3.

4.3. Modeling Solute Diffusion and Partition Parameters. *4.3.1. Comparison between Average and Microscopic Diffusion Coefficients.* The effect of the interphase structure on the average diffusion coefficient was studied as follows. Experimental fluorescence intensity profiles for R-phycoerythrin, $I(x, t)$, displayed for various x values in Figure 4, were modeled with eqs 9 and 12 which assume Fickian diffusion in two semi-infinite media and constant values of the diffusion coefficient between 0 and x. Good fits (solid lines in Figure 4) were obtained at each distance x, in spite of the fact that conditions of semi-infinite diffusion are not perfectly fulfilled in solution (weak decrease of fluorescent intensity, $I_w(t)$, and thus the corresponding concentrations, with time due to consumption by the gel). Approximate average values $\tilde{D}_g(x)$ are thus obtained for each value of x (Table 2).

Rigorous calculations were also performed (dashed lines in Figure 4) by numerical resolution of the second Fick's law taking into account the variation of D_g with x and using the experimental values of the interphase layer thickness (120 μm) and $D_g(x)$ profiles. The results with R6G (Figure 3) have shown that $D_g(x)$ profiles can be fitted with a parabolic function. For R-phycoerythrin, a similar parabolic function was fitted on the experimental points (inset in Figure 4). Constant values of $D_g(x)$ were used for $x \ge 120$ μm.

(28) Johansson, L.; Elvingson, C.; Löfroth, J. E. *Macromolecules* **1991**, *24*, 6024−6029.
(29) Clague, D. S.; Philips, R. J. *Phys. Fluids* **1996**, *8*, 1720−1731.
(30) Philips, R. J. *Biophys. J.* **2000**, *79*, 3350−3353.

Three interesting conclusions can be drawn from the results of the approximate and rigorous modeling.

(i) It can be seen that both models fit equally well the experimental data of Figure 4, despite the fact that the approximate model provides $\tilde{D}_g(x)$values which differ significantly from the true values, when x is not large enough (see below). Thus such fits are not very sensitive to the model used, and conclusions drawn should be done with care.

(ii) Table 2 shows that the $\tilde{D}_g(x)$ values obtained by the approximate model, for $x > 120\ \mu$m, are lower than experimental D_g(bulk) (Table 1). $\tilde{D}_g(x)$ tends to D_g(bulk) for $x = 1050\ \mu$m, but it is smaller at shorter distances, and the difference increases when $x \rightarrow 0$. Similarly, the value of $\tilde{D}_w$ ($x = -189\ \mu$m) is smaller than D_w. This is due to the fact that $\tilde{D}_g(x)$ has been considered as independent of x when integrating eq 5. Consequently it represents an average value of D_g between 0 and x. At low x values, $\tilde{D}_g(x)$ is thus strongly influenced by the interphase properties, while, when $x \rightarrow \infty$, the role of these properties becomes negligible, and $\tilde{D}_g(x) \rightarrow D_g$(bulk). The important result of Table 2 is that the simple Fick's law with constant D_g value (eqs 8−12) is applicable only for $x > 1000\ \mu$m, i.e., for gel thicknesses ∼10 times larger than the interphase layer. For smaller x values, it leads to significant underestimation of the diffusion coefficient.

(iii) On the opposite, Table 2 shows that the approximate model provides constant K values, independent of x. The average K value calculated for R-phycoerythrin (0.59 ± 0.02) is in agreement with those obtained from laser interferometry for solutes with similar sizes such as pullulans ($K = 0.76-0.57$, $R_h = 2-8$ nm) and bovine serum albumin ($K = 0.59$, $R_h = 3.59$ nm).[31] Thus correct K values are obtained, irrespective of x, even with the approximate model.

4.3.2. Effect of the Interphase Structure on Solute Transport in Gel: Analytical and Environmental Implications. A number of analytical/environmental problems are related to the diffusion of solutes in hydrogels. Understanding the nutrients supply inside biofilms is a major environmental example. Interpretation of in situ metal speciation with DGT, or voltammetry,[5] or in situ analysis of O_2, and many other nutrients[5] are largely based on chemical sensors or biosensors in which the sensing part is separated from the environmental (aquatic) medium by hydrogels (usually agarose or polyacrylamide gels). Typically, interpretations are based on the idea that the gel is homogeneous and D_g is independent of x. The present results suggest that this assumption might not always be valid.

The importance of the interphase effects on the flux of solute through a gel layer is tested theoretically, with a simple case explained below and in Figure 6. A diaphragm diffusion cell is considered where a receiving solution is separated from the test solution by a gel membrane with variable thickness. Prior to an experiment, the gel membrane is installed in the diffusion cell and left to equilibrate with the two aqueous electrolyte solutions, under constant stirring. At the beginning of the transport experiment, the solute is introduced in the source cell and at given time-intervals an aliquot of solution is taken out from each compartment for quantitative analysis. Typically the gel thickness ranges from a few hundred μm to a few mm. The interphase layer is assumed to have the same characteristics as in Figure 3 (thickness $= 120\ \mu$m; $D_g(0) \sim D_g$(bulk)/2). Gel interphase layers are supposed to exist on both sides of the membrane. The solute flux, J, through the membrane with its two interphase layers (see inset of Figure 6) is normalized by the flux, J_0, which would be obtained with a fully homogeneous gel membrane (no interphase layers with specific characteristics) with the same overall thickness. Computations have been performed for two compounds with different diffusion coefficients in bulk gels: $D_g = 2.64 \times 10^{-6}$ cm^2 s^{-1} (corresponding to $R_h = 0.76$ nm), and $D_g = 3.87 \times 10^{-7}$ cm^2 s^{-1} (corresponding to $R_h = 4.6$ nm). Figure 6 shows that the difference between J and J_0 is not larger than 5%, only when membrane thicknesses are larger than 0.8 and 1.5 mm, respectively. This is larger than many gel membranes typically used in practice for sensors and similar to biofilm thicknesses.

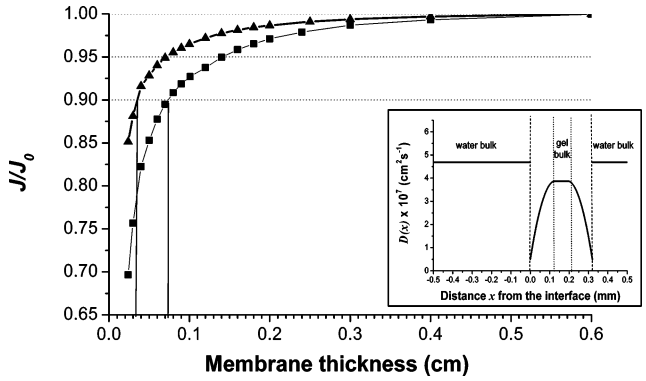

Figure 6. Ratio of the solute fluxes J and J_0 across the gel membrane as a function of the membrane thickness. J_0 = flux computed by assuming that $D_g(x)$ is independent of x (interphase properties = bulk properties). J = flux computed based on the scheme in the inset. The thicknesses of the two interfaces layers are 120 μm; $K = 1$, independent of x. (▲) R6G, D_g(bulk) $= 2.64\ 10^{-6}$ cm^2 s^{-1}, $R_h = 0.76$ nm; (■) R-phycoerythrin, D_g(bulk) $= 3.87\ 10^{-7}$ cm^2 s^{-1}, $R_h = 4.6$ nm. Inset: $D_g(x)$ profile used for R-phycoerythrin. For R6G the same profile shape was used, but with values of Figure 5.

In a number of analytical applications, the effect of the interphase layer may be corrected for by the calibration procedure used, provided gel preparation is reproducible enough. In addition, the effect observed here with agarose, might be weaker or nonexistent with different types of hydrogels. In particular gels based on covalent bonds, like polyacrylamide gels, may behave differently from those based on aggregation of fibers (like agarose). The latter however are important in environmental systems, like biofilms. Comparison of interfacial properties of different types of gel would certainly be very useful. But anyway, these results strongly suggest that the possible nonhomogeneous structure of hydrogels should be carefully considered before interpreting environmental or analytical data.

5. Concluding Remarks

A few important conclusions can be derived from the present fluorescence correlation spectroscopy study.

Interphase layers on water and gel sides of the interface: FCS measurements show that layers with specific properties are formed on both side of the interphase. The layer on the gel side ensures a key sieving role of solutes (see below). On the water side, a layer of ∼30 nm is observed, whose viscosity is significantly larger than in water, probably due to semi-free agarose fibers extending in the water phase.

Porosity of the gel water interface: On the basis of the diffusion properties of solutes, it has also been shown that the structure of gel/water interface is different from that in the bulk gel. A gel interphase layer of ∼120 μm thickness was observed, whose porosity is significantly lower than that in the bulk gel with fiber density of 1.5 wt %. The porosity decreases from the bulk gel to the gel/water interface down to a porosity equivalent

(31) Roger, P.; Mattison, C.; Axelson, A.; Zacchi, G. *Biotechnol. Bioengin.* **2000**, *69*, 654−663.

to that of a 5−6 wt % gel. Such a local denser structure could be due either to a larger fiber concentration or to a more entangled fiber organization in the interphase. For steric reasons, diffusion coefficients of nanometric solutes are reduced in this layer, and it also serves as a sieve which hinders penetration, from solution to the gel, of particles with radius larger than ∼15 nm. This critical size is significantly lower than the maximum radius (70 nm) of particles which can move in interconnected pores in the bulk gel. The interphase porosity is thus the key parameter which controls the penetration of solutes from the solution to the gel.

Average and microscopic diffusion coefficients: The contribution of the thin interphase to the average flux of a solute through the gel can only be neglected at sufficiently large time (min−h) and spatial (> mm) scales of observation. Experimental and modeling results suggest that for the interphase layer studied in this paper (120 μm), a minimum gel thickness of 1−2 mm is required for its role to be negligible. When this is achieved, for all the solutes studied, the average macroscopic diffusion coefficients calculated are in agreements with those measured at the microscopic scale by FCS in the bulk gel. FCS measurements with several solutes with radius ≤14 nm (i.e., significantly lower than the critical maximum size in the bulk gel) showed that, in all these cases, normal diffusion theory related to classical Fick's law can be used.

Acknowledgment. The authors acknowledge very gratefully Dr. K. Startchev for his helpful contribution on the polydispersity measurements from FCS data. This work was supported by Grants 20-61871.00 and 200020-101974/1 from the Swiss National Science Foundation.

LA0611155